Shielding of a moving test charge in a quantum plasma

D. Else, R. Kompaneets, and S. V. Vladimirov

School of Physics, The University of Sydney, Sydney, New South Wales 2006, Australia

The linearized potential of a moving test charge in a one-component fully degenerate fermion plasma is studied using the Lindhard dielectric function. The motion is found to greatly enhance the Friedel oscillations behind the charge, especially for velocities larger than half of the Fermi velocity, in which case the asymptotic behavior of their amplitude changes from $1/r^3$ to $1/r^{2.5}$. In the absence of the quantum recoil (tunneling) the potential reduces to a form similar to that in a classical Maxwellian plasma, with a difference being that the plasma oscillations behind the charge at velocities larger than the Fermi velocity are not Landau damped.

I. INTRODUCTION

The Debye shielding of a moving test charge in a classical plasma is one of the most fundamental problems in plasma physics [1–15]. In the collisionless case the motion is known to result in the $1/r^3$ dependence of the potential at large distances [4]. The angular dependence of this asymptotic form is determined by the velocity distributions of the plasma components [4]; and, for instance, for a one-component Maxwellian plasma the potential is repulsive (for a particle of like charge) in front of the test charge and attractive behind it and perpendicular to the motion [5,10,16]. In addition, behind the charge a large number of potential minima are formed at substantially suprathermal velocities [1,10,16]. The presence of collisions can lead to the $1/r^2$ dependence of the potential [8], while the excitation of ion-sound waves can result in the formation of an oscillatory wake structure inside the corresponding Mach cone [12–14].

While the above studies deal with classical plasmas, recently there has been a rapidly growing interest in quantum plasmas, motivated primarily by the development of nano-structured metallic and semiconductor materials [17–24]. Much attention has been given to a one-component weakly coupled fully degenerate fermion plasma [25–35]. Such a plasma is often described by the Lindhard dielectric function [30,36] where the only quantum effects included are the degeneracy and the quantum recoil (tunneling). It can be derived using the Wigner-Poisson system [18,34,37–41], a quantum analog of the Vlasov-Poisson system.

We present an investigation of the shielding of a moving classical charge in a quantum plasma using the Lindhard dielectric function. The free parameters in this model are the velocity of the test charge in units of the Fermi velocity and the plasma coupling parameter. The latter governs the role of the quantum recoil and should be small for the model to apply, as discussed in Sec. IV. In the limit of zero coupling parameter (i.e., in the absence of the quantum recoil) the potential is semiclassical in the sense that it can be found using the classical approach but with a degenerate velocity distribution [34]. Such a potential has the aforementioned $1/r^3$ asymptote at large distances and was investigated in Ref. [42] at small velocities. At a finite coupling parameter but zero velocity the potential is known to have Friedel oscillations [30,43]. Our study extends these results to the gen-

eral case of arbitrary velocity and coupling parameter and shows how the quantum recoil changes the semiclassical potential and how the motion modifies the Friedel oscillations.

II. MODEL

The potential around a point test charge Q moving at a constant velocity $\mathbf{v}$ in a three-dimensional plasma is given in the linear approximation by the formula [4,30,44]

$$\varphi(\mathbf{r}) = \frac{Q}{4\pi\epsilon_0}\frac{1}{2\pi^2}\int\frac{\exp(i\mathbf{k}\cdot\mathbf{r})}{k^2 D(\mathbf{k}\cdot\mathbf{v},\mathbf{k})}d\mathbf{k}, \quad (1)$$

where $\mathbf{r}$ denotes the position relative to the instantaneous position of the charge, ϵ_0 is the electric constant, and $D(\omega,\mathbf{k})$ is the dielectric function of the plasma. We take the screening to be due to the response of a single fully degenerate plasma component (e.g., electrons), with all the other components remaining fixed as a homogeneous neutralizing background. To describe their response, we use the Lindhard dielectric function [27,29,30,32,36]

$$D(\omega,\mathbf{k}) = 1 + \frac{m\omega_p^2}{\hbar n k^2}\int\frac{f(\mathbf{p}+\hbar\mathbf{k}/2)-f(\mathbf{p}-\hbar\mathbf{k}/2)}{\omega+i\nu-\mathbf{k}\cdot\mathbf{p}/m}d\mathbf{p}, \quad (2)$$

where $\omega_p = \sqrt{ne^2/(\epsilon_0 m)}$ is the plasma frequency; n is the particle number density (of the component that responds to the test charge); e and m is their charge and mass, respectively; ν is an infinitesimal positive number (i.e., the limit $\nu\to 0^+$ should be taken); and $f(\mathbf{p})$ is the three-dimensional Fermi-Dirac distribution function

$$f(\mathbf{p}) = \begin{cases} 2\left(\dfrac{1}{2\pi\hbar}\right)^3 & \text{if } |\mathbf{p}| < p_F \\ 0 & \text{if } |\mathbf{p}| > p_F, \end{cases} \quad (3)$$

where $p_F = \hbar(3\pi^2 n)^{1/3}$ is the Fermi momentum and $\hbar$ is the Planck constant over 2π. The applicability of the model is discussed in Sec. IV.

Carrying out the integral in Eq. (2) gives [30,36]

$$D(\omega,\mathbf{k}) = 1 + \frac{1}{k^2\lambda_{TF}^2}\frac{1}{2a}[F(\omega+i\nu+a,k)-F(\omega+i\nu-a,k)],$$

$$(4a)$$

where

$$a = \frac{\hbar k^2}{2m}, \tag{4b}$$

$$F(\Omega, k) = \frac{\Omega}{2} + \frac{(kv_F)^2 - \Omega^2}{4kv_F} \ln\left(\frac{\Omega + kv_F}{\Omega - kv_F}\right), \tag{4c}$$

$v_F = p_F/m$ is the Fermi velocity, and $\lambda_{TF} = v_F/(\omega_p\sqrt{3})$ is the Thomas-Fermi screening length; the principal branch of the complex logarithm should be taken.

Unless otherwise stated, the figures in this paper have been generated by numerical integration of Eq. (1) using the dielectric function (4). We choose the free parameters to be the degenerate Mach number $M = v/v_F$ and the parameter

$$\eta = \frac{\hbar \omega_p}{4E_F}, \tag{5}$$

where $E_F = p_F^2/(2m)$ is the Fermi energy. Note that the parameter η is related to the plasma coupling parameter $\Gamma = e^2 n^{1/3}/(4\pi\epsilon_0 E_F)$ via

$$\eta = \sqrt{\frac{\pi\Gamma}{2(3\pi^2)^{2/3}}}. \tag{6}$$

In Appendix A, we have reformulated the problem in nondimensional form in terms of the free parameters η and M.

III. RESULTS

A. Semiclassical limit

We first consider the semiclassical limit $\eta \to 0$, where the degeneracy of the unperturbed state is the only quantum effect. The extent to which the results of the present subsection are relevant despite the fact that we neglect relativistic effects is discussed in Sec. IV. In the semiclassical limit we have [31]

$$D(\mathbf{k}\cdot\mathbf{v}, \mathbf{k}) = 1 + \frac{1}{k^2\lambda_{TF}^2} G(M\hat{\mathbf{k}}\cdot\hat{\mathbf{v}}), \tag{7}$$

where the hat denotes unit vectors,

$$G(x) = 1 - \frac{x + i\epsilon}{2} \ln\left(\frac{x + i\epsilon + 1}{x + i\epsilon - 1}\right), \tag{8}$$

and ϵ is an infinitesimal positive number. If we set $v = 0$ we get the exponentially screened potential of the Debye form:

$$\varphi(\mathbf{r}) = \frac{Q}{4\pi\epsilon_0 r} \exp\left(-\frac{r}{\lambda_{TF}}\right). \tag{9}$$

Now, for $M < 1$, the reciprocal dielectric function $1/D(\mathbf{k}\cdot\mathbf{v}, \mathbf{k})$ does not have singularities at real $\mathbf{k}$ and, hence, as shown in Ref. [4], the asymptotic potential as $r \to \infty$ is

$$\varphi(\mathbf{r}) = \frac{Q}{4\pi\epsilon_0} H(\gamma) \frac{\lambda_{TF}^2}{r^3} + O\left(\frac{1}{r^5}\right), \tag{10}$$

where γ is the angle between $\mathbf{r}$ and $\mathbf{v}$, and [45]
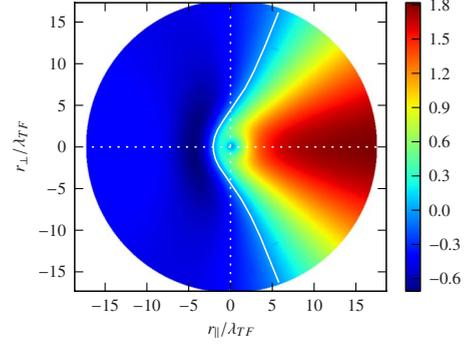
FIG. 1. (Color online) The quantity φr^3 [in units of $Q\lambda_{TF}^2/(4\pi\epsilon_0)$] in the semiclassical case ($\eta \to 0$), with the test charge at the origin and moving at speed $v = 0.5v_F$ to the right. The white superimposed curve denotes the boundary between positive and negative potentials (for $Q > 0$, the positive potential is on the right of the figure).

$$H(\gamma) = -\frac{i}{\pi^2} \lim_{\delta \to 0^+} \int_0^{2\pi} d\phi \int_{-1}^1 d\mu$$

$$\times \frac{1}{G[M(\mu\cos\gamma + \sqrt{1-\mu^2}\sin\phi\sin\gamma)]}$$

$$\times \frac{1}{(\mu + i\delta)^3}. \tag{11}$$

As $M \to 0$, we can expand $H(\gamma)$ in powers of M, giving the asymptotic formula

$$\varphi(\mathbf{r}) = \frac{Q}{4\pi\epsilon_0 r} \exp\left(-\frac{r}{\lambda_{TF}}\right) + \frac{Q}{4\pi\epsilon_0} \frac{\lambda_{TF}^2}{r^3}\left[2M\cos\gamma \right.$$

$$\left. + \left(\frac{\pi^2}{4} - 1\right)M^2(3\cos^2\gamma - 1)\right]$$

$$+ O\left(\frac{M^3}{r^3}\right) + O\left(\frac{M}{r^5}\right), \tag{12}$$

as $r \to \infty$, $M \to 0$. The term linear in M in Eq. (12) was given in [42], although they appear to be missing the factor of 2. This asymptotic result is qualitatively identical (the only difference is in the numerical coefficients in front of the two terms) to the classical case of a Maxwellian plasma [5]. Equation (12) shows that for small nonzero M, an attractive (for like charges) potential forms antiparallel and perpendicular to the motion, whereas the potential parallel to the motion remains repulsive (but decays as $1/r^3$ instead of exponentially as for $M = 0$). These features persist at velocities up to and including the Fermi velocity, as illustrated in Figs. 1 and 2. (Note that although Fig. 1 exhibits a cone-shaped feature in front of the charge, this is not an oscillatory Mach cone of the kind that occurs behind fast-moving charges and is shown in Fig. 3.)

On the other hand, for $M > 1$, the reciprocal dielectric function $1/D(\mathbf{k}\cdot\mathbf{v}, \mathbf{k})$ has a pole for real $\mathbf{k}$ [the parameter ϵ sets the rule for avoiding this pole in integral (1)]. Physically, this corresponds to the fact that a test charge moving faster than the Fermi velocity can excite plasma oscillations. Fur-
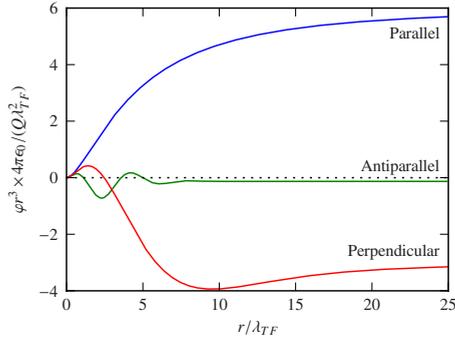
FIG. 2. (Color online) The quantity φr^3 [in units of $Q\lambda_{TF}^2/(4\pi\epsilon_0)$] in the semiclassical case, with the test charge moving at the Fermi velocity, in the directions parallel to the motion ($\hat{\mathbf{r}} \cdot \hat{\mathbf{v}} = 1$), perpendicular to the motion ($\hat{\mathbf{r}} \cdot \hat{\mathbf{v}} = 0$), and antiparallel to the motion ($\hat{\mathbf{r}} \cdot \hat{\mathbf{v}} = -1$).

thermore, since these oscillations have phase velocity greater than the Fermi velocity, they are not Landau damped, as can be seen mathematically in the fact that $D(\omega, k)$ has no imaginary part at $\omega/k > v_F$. This is because, with the unperturbed velocity distribution given by Eq. (3), there are no particles with velocities greater than v_F and hence no particles satisfying the resonance condition to contribute to Landau damping (this resonance condition is, since the quantum recoil disappears in the semiclassical limit, the same as in classical plasma physics) [31,32]. The result is a strong oscillatory wake (with amplitude decreasing as $1/r$) behind the test charge with an infinite number of minima, as shown in Fig. 3. Note that an oscillatory structure behind the charge is also present in the case of a Maxwellian distribution at substantially suprathermal velocities, but it is Landau damped [10]. As a result, the number of minima is finite (although very large) because the $1/r^3$ asymptote falls off slower than the exponentially damped amplitude of oscillations.

B. General case

1. Case of $0 \le v \le v_F$

As is well known [30], at nonzero η the static dielectric function $D(0, \mathbf{k})$ has a nonanalyticity (the "Kohn anomaly"
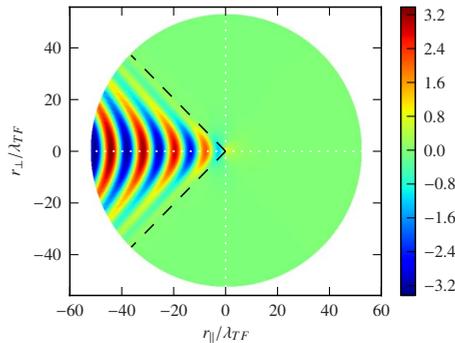
FIG. 3. (Color online) The ratio of the potential $\varphi(\mathbf{r})$ to the unscreened Coulomb potential $Q/(4\pi\epsilon_0 r)$, in the semiclassical case with the test charge at the origin and moving at speed $v = 1.4v_F$ to the right. Also shown (dashed lines) is the "Mach cone," defined by $r_\parallel/|r_\perp| = -\sqrt{M^2 - 1}$.
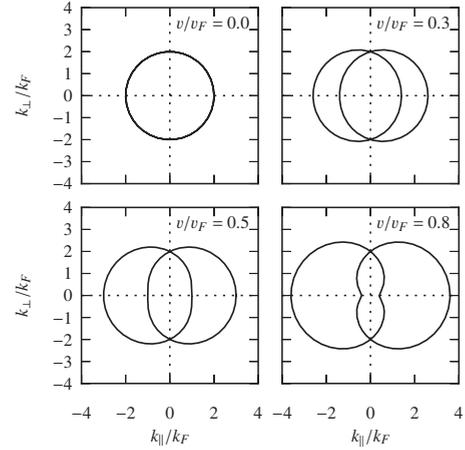
FIG. 4. The wave numbers $\mathbf{k}$ at which the Kohn anomaly in the dielectric function $D(\mathbf{k} \cdot \mathbf{v}, \mathbf{k})$ occurs; the velocity $\mathbf{v}$ is directed horizontally. This figure is valid for any value of η since the axes are normalized to the Fermi wave number k_F.

[46]) at wave numbers $|\mathbf{k}| = 2k_F$, where $k_F = p_F/\hbar$ is the Fermi wave number. The Kohn anomaly is related to the discontinuous Fermi surface and gives rise to the Friedel oscillations [47], with the potential as $r \to \infty$ given by [30]

$$\varphi(\mathbf{r}) = \frac{Q\lambda_{TF}^2}{4\pi\epsilon_0} \frac{36\eta^4}{(2+3\eta^2)^2} \frac{\cos(2k_F r)}{r^3} + o\left(\frac{1}{r^3}\right). \quad (13)$$

For nonzero velocities, the Kohn anomaly occurs at wave numbers $\mathbf{k}$ such that

$$|\mathbf{k}| = 2k_F(1 \pm M\hat{\mathbf{v}} \cdot \hat{\mathbf{k}}), \quad (14)$$

as illustrated in Fig. 4. The asymptotic potential as $r \to \infty$ is the superposition of the contribution from the Kohn anomaly and from the small wave numbers ($\mathbf{k} \to 0$); the latter is identical with the total semiclassical asymptotic potential since
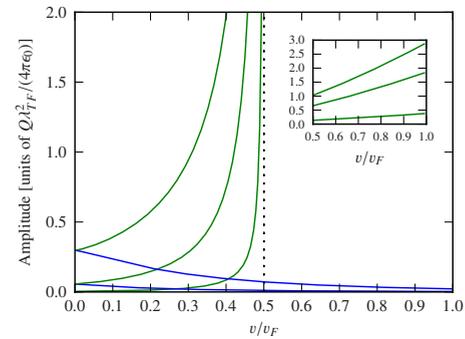
FIG. 5. (Color online) The amplitude of oscillations of the quantity φr^3 [in units of $Q\lambda_{TF}^2/(4\pi\epsilon_0)$], in the limit $r \to \infty$, behind the charge (green curves, increasing) and in front of the charge (blue curves, decreasing), as a function of test charge velocity, for values of η (in order of increasing amplitude): 0.15, 0.3, and 0.5. (The amplitude for $\eta = 0.15$ in front of the charge is too small to be visible on this graph.) Inset: the amplitude of oscillations of the quantity $\varphi r^{2.5}$ [in units of $Q\lambda_{TF}^{1.5}/(4\pi\epsilon_0)$] behind the charge, for $v/v_F > 0.5$.

the semiclassical and general forms of the dielectric function coincide in the limit $\mathbf{k} \to 0$.

In Appendix B, we outline the derivation of expressions for the asymptotic contribution resulting from the Kohn anomaly. The result is, for $\mathbf{r}$ and $\mathbf{v}$ parallel,

$$\varphi(\mathbf{r}) = \frac{Q}{4\pi\epsilon_0 r^3} \left\{ H(0)\lambda_{TF}^2 \right.$$
$$\left. + \frac{1}{2k_F \lambda_{TF}^2} \mathrm{Re}\left[f_+(1)\frac{\exp[2k_F(1+M)ir]}{1+2M} - f_+(0) \right] \right\}$$
$$+ o\left(\frac{1}{r^3}\right), \tag{15}$$

where the first term inside the curly brackets represents the semiclassical asymptotic contribution as described in Sec. III A, with $H(\gamma)$ given by Eq. (11), and the second term represents the contribution due to the Kohn anomaly, with

$$f_\pm(\mu) = \frac{1}{k_\pm^3[D(k_\pm v\mu, k_\pm)]^2}\left[\mu \mp \frac{2k_F M}{k_\pm}(1-\mu^2) \right]^2, \tag{16a}$$

$$k_\pm = 2k_F(1 \pm M|\mu|). \tag{16b}$$

For $\mathbf{r}$ and $\mathbf{v}$ antiparallel, we get a similar expression as long as $M < 1/2$:

$$\varphi(\mathbf{r}) = \frac{Q}{4\pi\epsilon_0 r^3} \left\{ H(\pi)\lambda_{TF}^2 \right.$$
$$\left. + \frac{1}{2k_F \lambda_{TF}^2} \mathrm{Re}\left[f_-(1)\frac{\exp[-2k_F(1-M)ir]}{1-2M} - f_-(0) \right] \right\}$$
$$+ o\left(\frac{1}{r^3}\right). \tag{17}$$

The difference between the two directions arises because, for $\mathbf{r}$ and $\mathbf{v}$ parallel, only the *outer* surface of the Kohn anomaly,
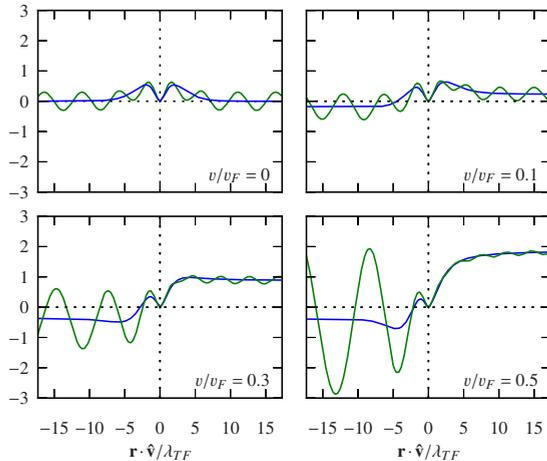
FIG. 6. (Color online) The quantity φr^3 [in units of $Q\lambda_{TF}^2/(4\pi\epsilon_0)$], along the direction of motion, in the semiclassical case (blue curves, nonoscillatory), and the case $\eta=0.5$ (green curves, oscillatory), at various velocities of the test charge.
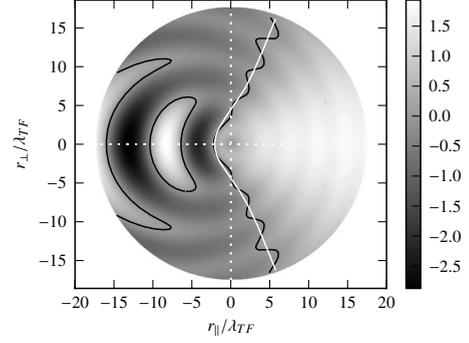
FIG. 7. The quantity φr^3 [in units of $Q\lambda_{TF}^2/(4\pi\epsilon_0)$] as a function of position for $\eta=0.5$, with the test charge at the origin and moving at speed $v=0.5v_F$ to the right. The black and white lines denote the boundary between positive and negative potentials for $\eta=0.5$ and the semiclassical case, respectively.

i.e., $|\mathbf{k}| = 2k_F(1+M|\hat{\mathbf{k}}\cdot\hat{\mathbf{v}}|)$, contributes to the asymptotic form; whereas, for $\mathbf{r}$ and $\mathbf{v}$ antiparallel, only the *inner* surface, i.e., $|\mathbf{k}| = 2k_F(1-M|\hat{\mathbf{k}}\cdot\hat{\mathbf{v}}|)$, contributes. Finally, for $\mathbf{r}$ and $\mathbf{v}$ antiparallel and $1/2 \leq M < 1$, a different asymptotic form emerges, with the amplitude of oscillations now decaying as $1/r^{2.5}$ rather than $1/r^3$:

$$\varphi(\mathbf{r}) = \frac{Q}{4\pi\epsilon_0} \sqrt{\frac{\pi}{M}} \frac{1}{2\lambda_{TF}^2 \sqrt{k_F} r^{2.5}} \mathrm{Re}\left[(1-i)f_-\left(\frac{1}{2M}\right) \right.$$
$$\left. \times \exp\left(-i\frac{k_F r}{2M}\right) \right] + o\left(\frac{1}{r^{2.5}}\right). \tag{18}$$

This is related to the change in concavity of the inner surface of the Kohn anomaly for $M > 1/2$, which can be observed in the last pane of Fig. 4. The velocity dependence of the amplitude of oscillations derived from Eqs. (15), (17), and (18) is shown in Fig. 5. It can be seen that, with increasing velocity, the Friedel oscillations become stronger behind the charge (especially for $M > 1/2$) and weaker in front. This is qualitatively illustrated in Figs. 6 and 7. Note, however, that no substantial change occurs in the Friedel oscillations in the direction perpendicular to the motion for any $v < v_F$.

When the test charge is moving at the Fermi velocity (see Figs. 8 and 9) the stronger Friedel oscillations are still
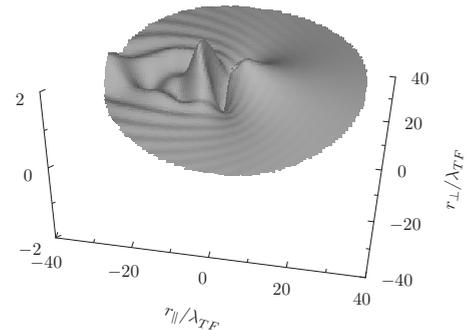
FIG. 8. The quantity φr^2 [in units of $Q\lambda_{TF}/(4\pi\epsilon_0)$] as a function of position in the case $\eta=0.5$, with the test charge located at the origin and moving to the right at the Fermi velocity v_F.

present behind the test charge in the far field, but close to the test charge a strong irregular wake field of a somewhat different character emerges. In particular, this near-field wake is still distinctly present even for very small values of η (e.g., $\eta = 0.02$).

2. Case of $v > v_F$

The inclusion of quantum recoil increases the lower bound on the phase velocity ω/k of undamped longitudinal oscillations [32]. This can be shown by numerically solving the equation $D(\omega,k) = 0$ for real ω and k, where $D(\omega,k)$ is given by Eq. (2) or its equivalent Eq. (3). The minimum phase velocity v_{thresh} is greater than the Fermi velocity, coinciding with it in the semiclassical limit, as shown in Fig. 10. Hence, for test charge velocities in the range $v_F < v < v_{\text{thresh}}$, the charge cannot excite undamped oscillations, and the wake depicted in Fig. 11 is formed. This is not as strong as in the semiclassical case (it falls off faster than $1/r$), and is also of a markedly different character, bearing no resemblance to a Mach cone.

For $v > v_{\text{thresh}}$, on the other hand, all undamped longitudinal oscillations with phase velocity $v_{\text{thresh}} < v_\phi < v$ are excited. We have not performed calculations for this case, but the results of Ref. [48] show a strong oscillatory wake, although its asymptotic behavior is not apparent. For very large velocities ($v \gg v_F$), the wake formed will be identical to the semiclassical wake [49].

IV. DISCUSSION

Let us discuss the applicability of the model. First, our model is based on the mean-field approximation which is justified at $\eta \ll 1$ [18,29,34]. In the limit $\eta \to 0$, however, the quantum recoil disappears [34]. Thus, the fact that our model includes the quantum recoil but does not include particle correlations makes it inconsistent in a certain sense. Nevertheless, it is widely used in the literature, i.e., at small η the quantum recoil is assumed to be more important than particle correlations. Their effects are discussed, e.g., in Refs. [29,50–53].

FIG. 10. The dependence of the threshold velocity v_{thresh} on the parameter η. In the region marked "undamped," undamped oscillations are excited. In the region marked "damped," they are not excited.

Second, our model does not include relativistic effects. This imposes a lower bound on the parameter η since the latter can be represented as

$$\eta = \sqrt{\frac{\alpha}{3\pi}\frac{c}{v_F}}, \qquad (19)$$

where c is the speed of light and $\alpha = e^2/(4\pi\epsilon_0 \hbar c) \approx 1/137$ is the fine-structure constant (here, we assumed that the charge of the particles is equal in its absolute value to the elementary charge). The condition $v_F \ll c$ requires $\eta \gg \sqrt{\alpha/(3\pi)} \approx 0.03$. Hence, the limit of $\eta \to 0$, as considered in Sec. III A, cannot be taken strictly. Nevertheless, the results of Sec. III A are relevant in a certain parameter regime. Indeed, the limit $\eta \to 0$ corresponds physically to the neglect of the quantum recoil, while the quantum recoil provides a contribution given approximately by Eq. (13) (for $M \ll 1$ and $r \gg \lambda_{TF}$). This is negligible compared to the $1/r^3$ term in Eq. (12) for $5\eta^4 \ll M$. (To be exact, the latter inequality is for $|\cos\gamma| \sim 1$, while for $\cos\gamma = 0$ it changes to $2\eta^2 \ll M$.) Thus, the applicability range of Eq. (12) due to the above restriction $\eta \gg 0.03$ is $4 \times 10^{-6} \ll 5\eta^4 \ll M \ll 1$ (again, it is for $|\cos\gamma| \sim 1$, while for $\cos\gamma = 0$ it changes to $2 \times 10^{-3} \ll 2\eta^2 \ll M \ll 1$). As the velocity increases, the effect of the quantum recoil becomes less important in front of the charge

FIG. 9. (Color online) The quantity φr^2 [in units of $Q\lambda_{TF}/(4\pi\epsilon_0)$] behind the test charge for $v = v_F$. Green curve is $\eta = 0.5$; red curve is $\eta = 0.02$; blue curve is semiclassical. The test charge is at the right of the figure ($r_\parallel = 0$). Inset: an extension of the main graph, for $\eta = 0.5$ (green curve) and $\eta = 0.3$ (magenta curve).
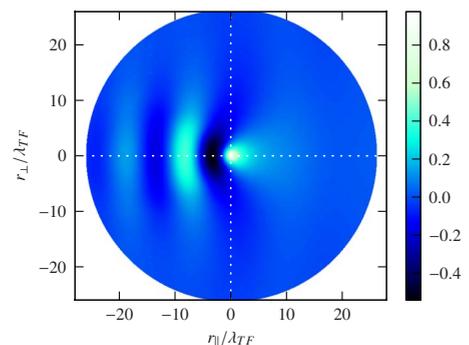
FIG. 11. (Color online) The ratio of the potential $\varphi(\mathbf{r})$ to the unscreened Coulomb potential $Q/(4\pi\epsilon_0 r)$, in the case $\eta = 0.5$, with the test charge at the origin and moving at speed $v = 1.4v_F$ to the right.

(such that for v/v_F not too close to zero the semiclassical and general forms of the potential are very similar even for $\eta = 0.5$, as can be seen in Fig. 6), and more important behind the charge, especially at $v/v_F > 0.5$.

Third, our model deals with the linearized potential. The linearization is justified when the potential energy of the interaction of a plasma particle with the test charge at the characteristic screening length (i.e., the length at which the Coulomb potential and the actual potential start to significantly deviate from each other) is much smaller than the characteristic kinetic energy of the particles in the frame of the test charge. At small velocities ($v \lesssim v_F$) this condition reads $|Qe|/(4\pi\epsilon_0\lambda_{TF}) \ll E_F$, which is equivalent to $12\pi(|Q/e|)\eta^3 \ll 1$, while at large velocities ($v \gtrsim v_F$) the characteristic screening length becomes v/ω_p and the above condition changes to $|Qe|\omega_p/(4\pi\epsilon_0 v) \ll mv^2$, which can be rewritten as $12\pi(|Q/e|)\eta^3(v_F/v)^3 \ll 1$. Thus, larger velocities imply better applicability of the linear theory.

Finally, there are a number of other effects which are not considered in our model but may be important under certain conditions. For instance, in our model the shielding is due to one plasma component (e.g., electrons) only. The screening in the presence of both electron and ion responses is considered in Refs. [54,55] using the quantum hydrodynamic model [34]. Furthermore, we did not include plasma production and loss processes. In classical plasmas they can introduce an additional nonscreened term and/or a weakly screened term in the potential and thus change its long-range behavior, even in the absence of the charge motion [56–59]. In quantum plasmas these processes (e.g., pair creation and annihilation) can have an important effect on the wave dispersion [60] and thus can affect the shielding of a moving charge.

The potential of a moving test charge under the Lindhard dielectric function has previously been investigated in Ref. [48]. That paper focused on the potential along the line of motion and surrounding the first potential minimum behind the test charge, for values of η approximately in the range 0.3–0.6, while the present paper is focused on the three-dimensional distribution and asymptotic behavior. Since the authors of Ref. [48] considered only the "wake potential," i.e., with the Coulomb potential subtracted, the actual behavior of the potential is not apparent from their work except when the wake is strong enough that the Coulomb potential is small by comparison, which occurs only when undamped oscillations are excited, i.e., $v > v_{thresh}$. We have not studied this case in the present paper.

Our results can be applied, for instance, to the investigation of bound electron states in the wake fields of ions in solids. This problem was studied in Ref. [48] using a parabolic fit to the potential around the first potential minimum, while a detailed investigation requires accurate knowledge of the whole potential distribution. Furthermore, our model can be extended to calculate the stopping power or the drag force, similar to classical plasmas [44,61–64].

V. CONCLUSION

We have studied the shielding of a moving classical test charge in a fully degenerate fermion plasma in both the semi-classical case (when the degeneracy of the unperturbed state is the only important quantum effect) and the case when quantum recoil is included. In the semiclassical case for $v \lesssim v_F$, the potential goes asymptotically as $1/r^3$, and is repulsive in front of the test charge and attractive behind the test charge and perpendicular to the motion; for v close to v_F the attraction is especially pronounced perpendicular to the motion. For $v > v_F$ the test charge excites plasma oscillations and a strong oscillatory wake is formed inside the Mach cone.

We have also found that the inclusion of quantum recoil leads to other effects entirely absent from the semiclassical case and the case of a Maxwellian distribution. The Friedel oscillations, already present in the screening of a static charge, are increased in strength behind a moving charge, and for $v > v_F/2$ the asymptotic behavior of their amplitude behind the charge changes from $1/r^3$ to $1/r^{2.5}$. Furthermore, the inclusion of quantum recoil makes the threshold velocity for excitation of an oscillatory wake of undamped plasma oscillations larger than the Fermi velocity. These findings extend the previous results on the shielding of a moving charge in a classical plasma to the quantum case and can be applied, for instance, to the investigation of bound electron states in the wake fields of ions in solids.

APPENDIX A: NONDIMENSIONAL FORM OF THE EQUATIONS

In order to demonstrate that our choice of free parameters M and η determines the potential up to scaling, we express the problem in nondimensional form in terms of these parameters. Defining the normalized wave number and frequency by $\mathbf{q} \equiv (v_F/\omega_p)\mathbf{k}$ and $w \equiv \omega/\omega_p$, the dielectric function of Eq. (4) can be written as

$$D(\omega,k) = \widetilde{D}(w,q) = 1 + \frac{3}{q^2}\frac{1}{2\,\eta q^2}[\widetilde{F}(w + i\widetilde{\nu} + \eta q^2, q)$$
$$- \widetilde{F}(w + i\widetilde{\nu} - \eta q^2, q)], \tag{A1a}$$

where $\widetilde{\nu} = \nu/\omega_p$ is an infinitesimal positive number, and

$$\widetilde{F}(W,q) = \frac{W}{2} + \frac{q^2 - W^2}{4q}\ln\left(\frac{W + q}{W - q}\right). \tag{A1b}$$

If we now define the normalized variables $\mathbf{x} \equiv \mathbf{r}/\lambda_{TF}$ and $\Phi \equiv (4\pi\epsilon_0\lambda_{TF}/Q)\varphi$, the nondimensionalized form of Eq. (1) becomes

$$\Phi(\mathbf{x}) = \frac{1}{2\pi^2\sqrt{3}}\int \frac{\exp(i\mathbf{q}\cdot\mathbf{x}/\sqrt{3})}{q^2\widetilde{D}(M\mathbf{q}\cdot\hat{\mathbf{v}},q)}d\mathbf{q}, \tag{A2}$$

where $\hat{\mathbf{v}}$ is the unit vector pointing in the direction of motion of the test charge.

APPENDIX B: DERIVATION OF EQS. (15), (16a), (16b), (17), and (18)

In order to derive the asymptotic contribution to the potential from the Kohn anomaly, we first integrate Eq. (1) by parts twice. The surface terms at $\mathbf{k}=0$ and at infinity vanish; in order to avoid having to evaluate surface terms at the locations of the Kohn anomaly, we take the limit $\nu \to 0^+$ only after integrating by parts. This leaves

$$\varphi(\mathbf{r}) = -\frac{Q}{4\pi\epsilon_0}\frac{1}{2\pi^2 r^2}\int\left[\left(\hat{\mathbf{r}}\cdot\frac{\partial}{\partial\mathbf{k}}\right)^2\left(\frac{1}{k^2 D(\mathbf{k}\cdot\mathbf{v},\mathbf{k})}\right)\right] \times \exp(i\mathbf{k}\cdot\mathbf{r})d\mathbf{k}. \quad \text{(B1)}$$

Assuming now that $\mathbf{r}$ is parallel or antiparallel to the motion, we can write

$$\int d\mathbf{k} \to 2\pi\int_{-1}^{1}d\mu\int_{0}^{\infty}k^2 dk, \quad \text{(B2)}$$

where $\mu=\hat{\mathbf{k}}\cdot\hat{\mathbf{v}}$. Replacing the integral over k with the asymptotic contribution thereto from the locations of the Kohn anomaly, $k=2k_F(1\pm M\mu)$, we obtain an intermediate expression, which we denote φ_{kohn}, for the asymptotic contribution to the potential from the Kohn singularity. For $\mathbf{r}$ and $\mathbf{v}$ parallel, this is

$$\varphi_{\text{kohn}}(\mathbf{r}) = i\frac{Q}{4\pi\epsilon_0}\frac{1}{2r^2\lambda_{TF}^2}\int_{-1}^{1}\left\{\frac{\text{sgn}(\mu)}{k_+^3[D(k_+v\mu,k_+)]^2}\right. \\ \left.\times\left[|\mu|-\frac{2k_F M}{k_+}(1-\mu^2)\right]^2\exp(ik_+r\mu)\right\}d\mu, \quad \text{(B3)}$$

where $k_+=2k_F(1+M|\mu|)$. Only the outer surface of the Kohn anomaly, i.e., $|\mathbf{k}|=k_+$, contributes to this expression; the contribution of the inner surface vanishes because it involves the integral $\int_{-\infty}^{\infty}e^{ix}/(x+i0)dx$, which evaluates to zero by closing the contour in the upper half-plane. For $\mathbf{r}$ and $\mathbf{v}$ antiparallel, on the other hand, we get

$$\varphi_{\text{kohn}}(\mathbf{r}) = -i\frac{Q}{4\pi\epsilon_0}\frac{1}{2r^2\lambda_{TF}^2}\int_{-1}^{1}\left\{\frac{\text{sgn}(\mu)}{k_-^3[D(k_-v\mu,k_-)]^2}\right. \\ \left.\times\left[|\mu|+\frac{2k_F M}{k_-}(1-\mu^2)\right]^2\exp(-ik_-r\mu)\right\}d\mu, \quad \text{(B4)}$$

where $k_-=2k_F(1-M|\mu|)$. This time only the inner surface, i.e., $|\mathbf{k}|=k_-$, contributes.

The asymptotic formulas given in the body of the paper, Eqs. (15), (16a), (16b), (17), and (18), follow from Eqs. (B3) and (B4) by changing the variable of integration to $\xi=\mu k_+(\mu)$ [in Eq. (B3)], or $\xi=\mu k_-(\mu)$ [in Eq. (B4)], and considering the asymptotic contribution as $r\to\infty$ from $\mu=\pm 1$ (the end points of the integration) and from $\mu=0$ (where the integrand is discontinuous). In addition, the stronger $\sim 1/r^{2.5}$ Friedel oscillations arise from points where $d\xi/d\mu=0$; this does not occur for $\mathbf{r}$ and $\mathbf{v}$ parallel, whereas for $\mathbf{r}$ and $\mathbf{v}$ antiparallel and $M\geq 1/2$, it occurs at $\mu=\pm 1/(2M)$.

[1] J. Neufeld and R. H. Ritchie, Phys. Rev. **98**, 1632 (1955).
[2] I. Oppenheim and N. G. van Kampen, Phys. Fluids **7**, 813 (1964).
[3] G. Joyce and D. Montgomery, Phys. Fluids **10**, 2017 (1967).
[4] D. Montgomery, G. Joyce, and R. Sugihara, Plasma Phys. **10**, 681 (1968).
[5] G. Cooper, Phys. Fluids **12**, 2707 (1969).
[6] E. W. Laingal, A. Lamont, and P. Fielding, J. Plasma Phys. **5**, 441 (1971).
[7] P. Chenevier, J. M. Dolique, and H. Peres, J. Plasma Phys. **10**, 185 (1973).
[8] L. Stenflo, M. Y. Yu, and P. K. Shukla, Phys. Fluids **16**, 450 (1973).
[9] C. Wang, G. Joyce, and D. R. Nicholson, J. Plasma Phys. **25**, 225 (1981).
[10] T. Peter, J. Plasma Phys. **44**, 269 (1990).
[11] E. E. Trofimovich and V. P. Krainov, Sov. Phys. JETP **77**, 910 (1993).
[12] S. V. Vladimirov and M. Nambu, Phys. Rev. E **52**, R2172 (1995).
[13] S. V. Vladimirov and O. Ishihara, Phys. Plasmas **3**, 444 (1996).
[14] O. Ishihara and S. V. Vladimirov, Phys. Plasmas **4**, 69 (1997).

[15] M. Lampe, G. Joyce, G. Ganguli, and V. Gavrishchaka, Phys. Plasmas **7**, 3851 (2000).
[16] R. Kompaneets, S. V. Vladimirov, A. V. Ivlev, and G. Morfill, New J. Phys. **10**, 063018 (2008).
[17] F. Haas, G. Manfredi, and M. Feix, Phys. Rev. E **62**, 2763 (2000).
[18] G. Manfredi, Fields Inst. Commun. **46**, 263 (2005).
[19] D. Kremp, M. Schlanges, and W.-D. Kraeft, *Quantum Statistics of Nonideal Plasmas* (Springer, Berlin, 2005).
[20] G. Manfredi and P. Hervieux, Appl. Phys. Lett. **91**, 061108 (2007).
[21] D. B. Melrose, *Quantum Plasmadynamics: Unmagnetized Plasmas* (Springer, Berlin, 2008).
[22] S. Ali, W. M. Moslem, I. Kourakis, and P. K. Shukla, New J. Phys. **10**, 023007 (2008).
[23] G. Brodin, M. Marklund, and G. Manfredi, Phys. Rev. Lett. **100**, 175001 (2008).
[24] P. K. Shukla, Nat. Phys. **5**, 92 (2009).
[25] I. I. Goldman, Zh. Eksp. Teor. Fiz. **17**, 681 (1947).
[26] V. P. Silin, Zh. Eksp. Teor. Fiz. **23**, 641 (1952).
[27] Y. L. Klimontovich and V. P. Silin, Zh. Eksp. Teor. Fiz. **23**, 151 (1952).
[28] D. Bohm and D. Pines, Phys. Rev. **92**, 609 (1953).

[29] Y. L. Klimontovich and V. P. Silin, Sov. Phys. Usp. **3**, 84 (1960).

[30] E. M. Lifshitz and L. P. Pitaevskii, *Physical Kinetics* (Pergamon, Oxford, 1981), pp. 161–167.

[31] A. F. Alexandrov, L. S. Bogdankevich, and A. A. Rukhadze, *Principles of Plasma Electrodynamics* (Springer, Berlin, 1984).

[32] V. S. Krivitskii and S. V. Vladimirov, Sov. Phys. JETP **73**, 821 (1991).

[33] S. V. Vladimirov, Phys. Scr. **49**, 625 (1994).

[34] G. Manfredi and F. Haas, Phys. Rev. B **64**, 075316 (2001).

[35] D. B. Melrose and A. Mushtaq, Phys. Plasmas **16**, 094508 (2009).

[36] J. Lindhard, K. Dan. Vidensk. Selsk. Mat. Fys. Medd. **28**, 1 (1954).

[37] E. Wigner, Phys. Rev. **40**, 749 (1932).

[38] V. I. Tatarskiǐ, Sov. Phys. Usp. **26**, 311 (1983).

[39] M. Hillery, R. F. O'Connell, M. O. Scully, and E. P. Wigner, Phys. Rep. **106**, 121 (1984).

[40] R. Diner, Transp. Theory Stat. Phys. **26**, 195 (1997).

[41] F. Haas, G. Manfredi, and J. Goedert, Phys. Rev. E **64**, 026413 (2001).

[42] P. K. Shukla, L. Stenflo, and R. Bingham, Phys. Lett. A **359**, 218 (2006).

[43] R. Grassme and P. Bussemer, Phys. Lett. A **175**, 441 (1993).

[44] A. V. Ivlev, S. A. Khrapak, S. K. Zhdanov, G. E. Morfill, and G. Joyce, Phys. Rev. Lett. **92**, 205007 (2004).

[45] R. Kompaneets, G. E. Morfill, and A. V. Ivlev, Phys. Plasmas **16**, 043705 (2009).

[46] W. Kohn, Phys. Rev. Lett. **2**, 393 (1959).

[47] J. Friedel, Nuovo Cimento, Suppl. **7**, 287 (1958).

[48] A. Mazarro, P. M. Echenique, and R. H. Ritchie, Phys. Rev. B **27**, 4117 (1983).

[49] D. H. Jakubassa, J. Phys. C **10**, 4491 (1977).

[50] R. A. Ferrell, Phys. Rev. **107**, 450 (1957).

[51] A. J. Glick, Phys. Rev. **129**, 1399 (1963).

[52] F. Toigo and T. O. Woodruff, Phys. Rev. B **2**, 3958 (1970).

[53] F. Toigo and T. O. Woodruff, Phys. Rev. B **4**, 4312 (1971).

[54] S. Ali and P. K. Shukla, Phys. Plasmas **13**, 102112 (2006).

[55] P. K. Shukla and B. Eliasson, Phys. Lett. A **372**, 2897 (2008).

[56] A. V. Filippov, A. G. Zagorodny, A. I. Momot, A. F. Pal, and A. N. Starostin, Sov. Phys. JETP **104**, 147 (2007).

[57] M. Chaudhuri, S. A. Khrapak, and G. E. Morfill, Phys. Plasmas **15**, 053703 (2008).

[58] S. A. Khrapak, A. V. Ivlev, and G. E. Morfill, Phys. Plasmas **17**, 042107 (2010).

[59] M. Chaudhuri, S. A. Khrapak, and G. E. Morfill, Phys. Plasmas **17**, 034503 (2010).

[60] J. McOrist, D. B. Melrose, and J. I. Weise, J. Plasma Phys. **73**, 495 (2007).

[61] T. Peter and J. Meyer-ter-Vehn, Phys. Rev. A **43**, 1998 (1991).

[62] A. V. Ivlev, S. K. Zhdanov, S. A. Khrapak, and G. E. Morfill, Phys. Rev. E **71**, 016405 (2005).

[63] S. A. Khrapak, A. V. Ivlev, S. K. Zhdanov, and G. E. Morfill, Phys. Plasmas **12**, 042308 (2005).

[64] S. A. Khrapak, M. Chaudhuri, and G. E. Morfill, IEEE Trans. Plasma Sci. **37**, 487 (2009).